Journal of Robotics and Control (JRC)
Volume 7, Issue 3, 2026
ISSN: 2715-5072, DOI: 10.18196/jrc.v7i3.27914

Spatial–Temporal Connectivity Descriptors for EEG-Based Mental Stress Detection Using Interpretable Machine Learning

Dwi Utari Surya [1], Sholeh Hadi Pramono [2]*, Panca Mudjirahardjo [3], Muhammad Aziz Muslim [4], Cries Avian [5], Mahdin Rohmatillah [6]
[1, 2, 3, 4,5,6] Department of Electrical Engineering, Universitas Brawijaya, Malang, Indonesia
[1] Department of Creative and Digital Industry, Universitas Brawijaya, Malang, Indonesia
Email: [1] d.utarisurya@ub.ac.id, [2]* sholehpramono@ub.ac.id, [3] panca@ub.ac.id, [4] muh_aziz@ub.ac.id, [5] cries.avian@ub.ac.id, [6] mahdin94@ub.ac.id
*Corresponding Author

Abstract— **Mental stress is a massive threat to global health because it has serious adverse effects on people's memory, emotional well-being, and productivity. Although electroencephalography (EEG) offers a non-invasive, high-temporal-resolution modality for stress assessment, the complex, non-stationary nature of stress-related neural responses remains a significant challenge for reliable EEG-based classification systems. The Research contribution is the development of an interpretable and modular EEG-based stress recognition framework that systematically integrates spatial–temporal connectivity descriptors with classical machine learning models. The proposed framework extracts handcrafted features from two complementary domains: temporal descriptors, including time-domain statistics and Hjorth parameters, and spatial connectivity measures, including inter-channel Pearson correlation, amplitude asymmetry, and Phase Lag Index (PLI). In addition, a log-transformed meta-correlation descriptor is introduced to capture nonlinear dependencies among temporal features. EEG signals from the DASPS dataset are segmented and evaluated using stratified 5-fold cross-validation across multiple classical classifiers. Experimental results demonstrate that the proposed framework achieves 99.18% accuracy and 99.89% AUC in binary stress classification using KNN, and 98.56% accuracy and 99.95% AUC in multiclass classification using SVM. Furthermore, XGBoost provides a favorable balance between accuracy and computational efficiency, achieving low inference latency (0.0015 s). These results confirm consistent performance across classifiers without reliance on deep learning architectures. Overall, the proposed framework offers an interpretable, low-latency solution for EEG-based mental stress detection, with strong potential for deployment in practical applications, such as wearable mental health monitoring systems and real-time stress assessment platforms.**

Keywords— EEG stress detection; spatiotemporal features; functional connectivity; handcrafted feature extraction; cross-validation; mental stress classification; affective computing

I. INTRODUCTION

Mental stress has become a widespread global issue with significant psychological, physiological, and socioeconomic consequences [1]-[2]. The World Health Organization states that a considerable number of people endure stress-related symptoms, with chronic stress considered one of the main risks for the development of cardiovascular diseases, anxiety, and depression [3]. In the fields of work, study, and healthcare, long-lasting stress has been associated with reduced productivity, impaired decision-making, memory loss, and lack of attention [4]. The modern lifestyle factors such as digital overload, economic insecurity, and social isolation not only aggravate these impacts but also contribute to the rising prevalence of stress among various populations [5]-[6]. Therefore, the non-invasive approach of neurophysiological monitoring via electroencephalography (EEG) is considered a key to reliable, timely stress detection, which, in turn, supports mental wellness and enables proactive health interventions [7]. EEG offers objective, real-time stress evaluation due to its high temporal resolution and sensitivity to changes in brain state, making this monitoring method highly promising [8], [9], [10].

The potential of EEG to recognize mental stress has been and continues to be a subject of significant Research; however, the complexity and fluctuations of brain dynamics still pose significant challenges for analytical purposes [11]. As a result of the massive intersubject differences, the variance of stress-related neural events over time, and the Influence of the surrounding context, these factors make it very hard to build a strong model [12]-[13]. On the other hand, some deep learning models, such as CNN-based architectures, EEGNet, and convolutional recurrent neural networks (CRNNs), have achieved strong and reliable results in EEG classification and emotion recognition tasks [14], [15], [16]. Nonetheless, deep learning methodologies still require complex training pipelines, the tuning of large parameter sets, and the use of non-trivial computational resources, which add to the overall cost [17]-[18]. These needs might pose significant constraints on their application in real-time or wearable EEG systems, where low latency, interpretability, and power efficiency are critical requirements [19]. The problem is even greater when low-cost, portable EEG devices are used, which are essential for monitoring stress in a scalable, practical manner; however, they limit the model's complexity and power consumption [20]. Therefore, even today, classic machine learning models are still a viable option for real-time EEG-based stress monitoring [21]-[22].

In recent years, researchers have examined a variety of methods for recognizing emotions and stress using EEG analysis. Deep neural networks, particularly convolutional and recurrent networks, have been widely used to extract hierarchical features from EEG signals. These networks often achieve perfect classification accuracy [23]-[24]. However, their drawbacks include the need for large amounts of data, long training times, and substantial computational power [17], [25], [26]. On the other hand, with the emergence of low-power deep learning architectures such as EEGNet and TinyML-based models, there is great potential to eliminate the computationally intensive stage of EEG analysis without loss of quality [16], [18], [27]. Despite these breakthroughs, deep learning techniques remain tied to traditional convolutional training and parameter tuning, which may lead to issues with interpretability, fixed latency, and deployment in low-resource settings [11]-[16]. On the other hand, the use of temporal features, spectral features, and inter-channel connectivity measures in handcrafted feature extraction methods can be considered a more complex yet physiologically meaningful approach, more appropriate for real-time EEG-based stress monitoring systems due to its lower computational complexity [28]-[29]. The works of [30] and [31] support the idea that by merging analyses of different features temporally and spatially, bio-signal analysis, including EMG and EEG, can be enriched. Techniques such as the Phase Lag Index (PLI), Pearson correlation, and amplitude asymmetry are suggested for studying the spatial dynamics of the brain.

Recent studies have continued to provide conclusive evidence that spatial connectivity features, such as correlation-based, coherence, and phase-synchronization measures, can be used to capture inter-regional communication patterns that decode stress and emotional states. To be specific, some of the latest Research has looked into the use of functional connectivity to improve the attention mechanism used in the cross-subject EEG emotion recognition and thereby connectivity integration improved generalization [32]; Besides that, the fusion of phase- and amplitude-based connectivity has been able to provide a better decoding of the emotional responses [33]; while the various methods of analyzing EEG connectivity during emotions have been suggesting the remarkable ability of spatial patterns to differentiate among emotions [34]. Besides that, the modeling of spatial–temporal connectivity has been frequently identified as a significant Research area in affective computing and stress-related EEG studies [35]-[36].

Even so, EEG signals are no more than implicit spatial and temporal dynamics that reflect affective neural activity through interchannel interactions and time-varying brain responses. Researchers have shown that integrating these domains produces better, more distinctive EEG representations for emotion analysis. To illustrate, STRFLNet, a spatio-temporal representation fusion learning network that effectively merges spatial dependencies and temporal evolution in EEG features, thereby increasing emotion recognition accuracy [37]. Similarly, a Dynamic Collaborative Evolutionary Network can interpret complex spatiotemporal relationships, thereby achieving strong generalization across diverse domains [38]. Additionally, DC-ASTGCN, which uses adaptive spatio-temporal graph convolution to model the directed relationships among channels, improves the decoding of emotional states [39]. On the whole, these studies argue that simultaneous modeling of spatial and temporal aspects is essential for revealing delicate neural patterns. Nevertheless, despite their effectiveness, deep learning-based spatio-temporal fusion methods are not suitable for real-time EEG stress monitoring applications due to their high reliance on large datasets, substantial computational resources, and limited interpretability.

Furthermore, logarithmic and nonlinear transformations have recently been used in EEG-based connectivity analysis to enhance the robustness of correlation distributions. Proper transformation of connectivity features improves stability in sensor-space EEG connectivity estimation [40]; on the other hand, nonlinear scaling enhances interpretability and discrimination in dynamic functional connectivity modeling [41]. Besides, the necessity of normalization and transformation to reduce the variability in EEG-based connectivity measures [42]-[43]. Likewise, logarithmic transformations in functional connectivity-based emotion decoding are used to maintain balanced dynamic ranges and improve classifier performance [43]. These transformation techniques not only render the connectivity distributions uniform but also allow handmade descriptors to prove their superiority.

EEG features are highly dimensional and are derived from spatial and temporal connectivity descriptors. For the above reason, classical machine learning models are compelling for structured data with a small number of samples. In small EEG datasets, traditional machine learning methods often outperform deep learning methods because they generalize better and are less computationally intensive [43]. By the same token, feature reduction combined with classical classifiers such as SVM and KNN improved emotion recognition accuracy on small EEG feature sets [44]. On top of that, conventional models remain very effective at generalization and are more reliable than deep learning architectures in structured EEG domains [45]. Because of these benefits, classical machine learning classifiers are used in this Research to examine the discriminative power of handcrafted spatial-temporal features while still maintaining computational efficiency.

The growing interest in connectivity-driven and deep fusion approaches has led to a relatively small number of studies that use handcrafted, interpretable frameworks to systematically integrate spatial-temporal connectivity measures with classical learning paradigms for EEG-based stress detection. However, the present study highlights the systematic integration of connectivity-based descriptors into a unified and interpretable handcrafted framework for stress detection [46]. Moreover, previous assessments are often limited to single-setting classification analyses that focus on binary stress discrimination, thereby providing an inadequate understanding of the model's performance across different stress intensity levels [47]-[48].

To overcome these difficulties, the current Research presents a distinctive Spatial–Temporal Connectivity Descriptor (STCD) for EEG-based stress detection. The main aims are to create a flexible feature extraction pipeline that combines the time descriptors (statistical measures and Hjorth parameters) with the spatial connectivity metrics (correlation, amplitude asymmetry, and PLI), to test the performance using eight traditional machine learning classifiers for both binary and multiclass stress classification, and to examine the balance between the accuracy of the classification and the delay in processing for real-time usability. The contributions of this work are threefold: i) the establishment of a cohesive and easily understood EEG-based stress recognition framework using handmade spatial-temporal descriptors; (ii) an all-around assessment of eight traditional machine learning models in both binary and multiclass settings, in terms of accuracy, inference latency, and training efficiency; (iii) a comparative performance analysis against the previous state-of-the-art methods on the DASPS dataset. These contributions from the current Research paper provide a practical approach to developing EEG-based mental stress detection systems that are both affordable and scalable.

To facilitate the proposed framework, Fig. 1 presents a conceptual overview of the spatial–temporal connectivity-based stress recognition pipeline, summarizing the main processing stages from EEG acquisition to classification and evaluation.

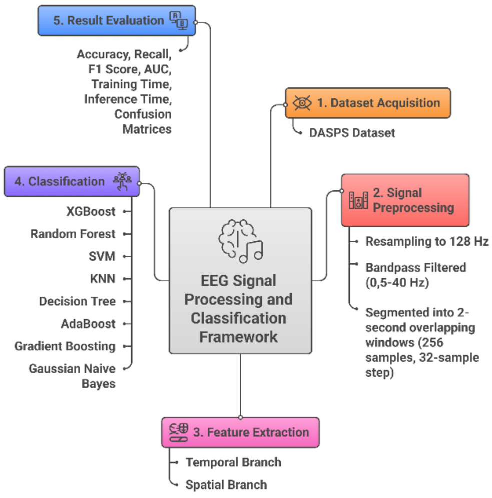

Fig. 1. Conceptual overview of the proposed spatial–temporal connectivity.

II. METHODOLOGY

The STCD system is suggested for EEG-based mental stress classification, as shown in Fig. 2. The workflow includes EEG acquisition and preprocessing, and the production of handcrafted temporal features and spatial connectivity descriptors. The resulting feature set is evaluated using multiple classical machine learning classifiers to perform both binary and multiclass stress classification.

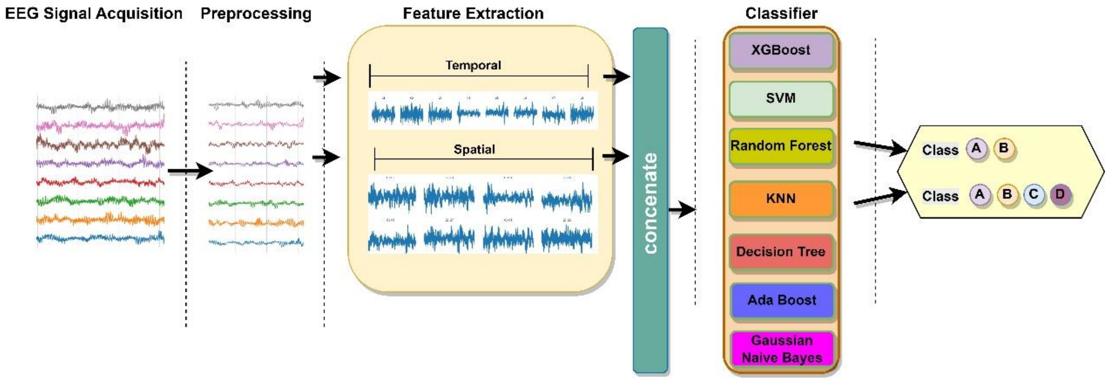

Fig. 2. Schematic of the STCD framework: EEG windows are processed to extract temporal and spatial features

A. Dataset

This Research revolves around the Database for Stress Processing under Simulated Conditions (DASPS), a public EEG dataset designed for the classification of anxious and stress states, among others. The DASPS dataset has been a standard for EEG-based stress recognition over the years, mainly because of its controlled experimental protocol and validated psychological labeling. The recordings in the dataset come from 23 healthy participants (12 men, 11 women; aged 18–35 years), who viewed audiovisual stimuli with emotional content in a laboratory under controlled conditions, as shown in Figure 3.

EEG signals were acquired using the Emotiv EPOC+ headset, which features 14 electrodes placed according to the international 10–20 system (AF3, F7, F3, FC5, T7, P7, O1, O2, P8, T8, FC6, F4, F8, AF4) with a sampling rate of 128 Hz. Every participant completed 12 trials, each associated with one stimulus of a different emotional nature: neutral, low-stress, or high-stress. The stimuli were taken from the databases, i.e., IAPS, IADS, which are known to elicit emotions and lasted about 60 seconds per trial [15].

This DASPS dataset was collected in accordance with approved ethical procedures, and all participants provided informed consent. Moreover, the stress labels were confirmed with standardized psychological tools such as HAM-A and SAM. For the binary and multiclass stress labels, valence-arousal scores were used based on the original DASPS annotation protocol, which comprised threshold-based partitioning to indicate relative affective intensity. This has become a widely used method among EEG researchers in the field of affective computing, as it reflects self-reported emotional states rather than clinically certified stressors. However, just like most of the laboratory-based EEG datasets, the demographic range and recording conditions of DASPS might limit its generalization to different real-world populations, and hence, further validation on additional datasets may be required in future studies.

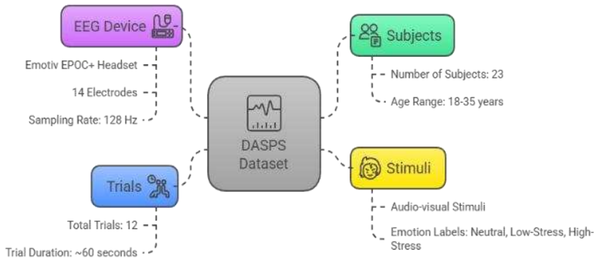

Fig 3. Overview of the DASPS Dataset Components

B. Algorithmic Workflow of STCD

The presented framework, STCD, proposes a Spatial–Temporal Connectivity Descriptor (STCD) that provides a complete outline of the signal processing and classification workflow. The framework comprised a systematic activity that started with segmenting the multichannel EEG signals, followed by placing them in overlapping windows. From each window, handcrafted temporal features, comprising statistical descriptors and Hjorth parameters, and spatial features such as Phase Lag Index (PLI), amplitude asymmetry, and Pearson correlation, are extracted and concatenated into a unified vector. To capture higher-order relationships, a meta-correlation descriptor is computed by correlating the original feature vector with its logarithm, yielding an enriched representation.

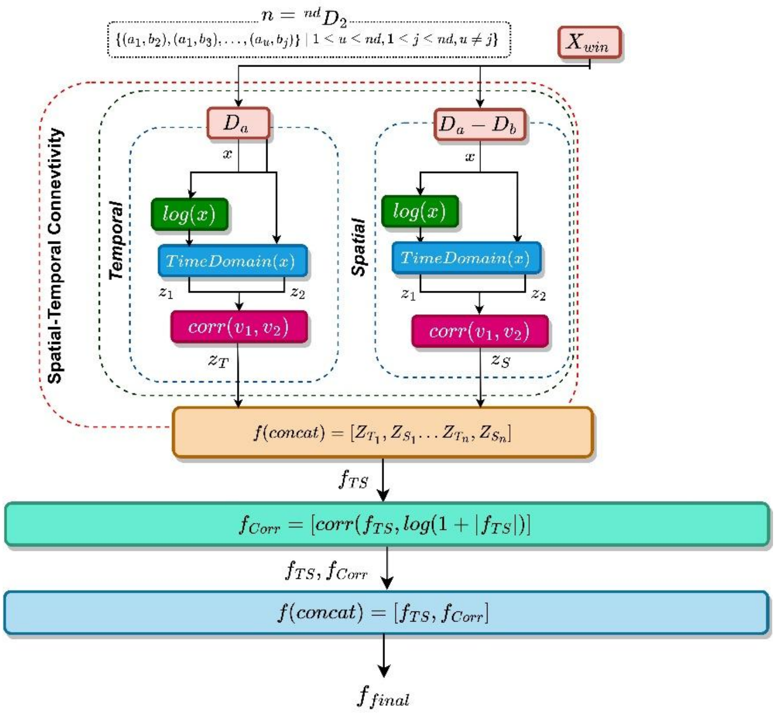

Fig. 4 Overview of the STCD feature extraction and classification pipeline, illustrating Spatial-Temporal Connectivity Descriptor computation and meta-correlation integration.

This final feature set is then used to train multiple classical classifiers, including XGBoost, SVM, Random Forest, and others, with a stratified 5-fold cross-validation scheme. Model performance is assessed using standard metrics such as accuracy, recall, F1-score, AUC, Training and Inference Time. Algorithm 1 presents the overall workflow of the proposed method, which can be summarized as follows:

- EEG signals are acquired and preprocessed using bandpass filtering and artifact inspection.
- The preprocessed EEG is segmented into fixed-length windows for feature extraction.
- Temporal descriptors, including statistical measures and Hjorth parameters, are computed for each channel.
- Spatial connectivity descriptors, including correlation-based, amplitude asymmetry, and phase-lag index measures, are extracted to capture inter-channel interactions.
- Temporal and spatial features are integrated into a unified feature representation.
- The resulting feature vectors are classified using multiple classical machine learning models under binary and multiclass stress recognition settings.
- Model performance is evaluated based on classification accuracy, latency, and training efficiency

ALGORITHM I: STCD EEG FEATURE EXTRACTION AND CLASSIFICATION

Step	Procedure
1	Input : EEG signals x: $\mathbb{R}^{n \times c \times t}$ where: n = number of trials, c = number of channels (electrodes), t = number of time points per trial
2	Output : Feature matrix f_final ∈ $\mathbb{R}^{n \times f}$ where f is number of extracted features
3	Segment EEG data using sliding window (length = 256, step = 32)
4	for i=1 to n: // For each trial
5	x_{trial}← x[i, :, :]
6	for ch=1 to c: // Per channel
7	Normalizex_{ch} ← $Standardscaler\ (x_{trial}[ch])$
8	Compute temporal features: - mean, std, skewness, kurtosis
9	- Hjorth activity, mobility, complexity
10	Store channel-wise features as temporal vector
11	End for
12	for each channel pair (a,b), a<b:
13	Compute $PLI_{a,b}$ ← $PhaseLagIndex\ (x_a, x_b)$
14	Compute amplitude asymmetry $Asym_{a,b} \leftarrow \mu_a, \mu_b$
15	Compute Pearson correlation between channel features
16	Compute log-transformed correlation
17	End for
18	Concatenate all temporal and spatial features: f_{TS}
19	Compute meta-correlation: f_{Corr} ← Corr (f_{TS}, log (1 + $\|f_{TS}\|$))
20	Concatenate all features f_{concat} = [f_{TS}, f_{Corr}]
21	Assign $f_{final}[i,:]$ ← f_{concat}
22	End for
23	Normalize features via StandardScaler
24	Train classifiers (XGB, RF, SVM, KNN, DT, AdaBoost, Gradient Boost, Naive Bayes) using stratified 5-fold cross-validation
25	Output: Accuracy, Recall, F1-Score, AUC, and inference time

C. Signal Preprocessing

Previous DASPS-based studies have commonly adopted window-based EEG segmentation and cross-validation to evaluate stress recognition models. The present work follows these established protocols, ensuring methodological consistency and comparability [47], [49], [50].

Raw EEG signals were first resampled to a uniform 128 Hz to ensure consistency across subjects. To preserve temporal resolution while enabling efficient processing, the signals were segmented into overlapping windows of 256 samples (equivalent to 2 seconds), with a step size of 32 samples [51]-[52]. Artifact removal was performed using a Butterworth bandpass filter (0.5–40 Hz) [53]. Additionally, a visual inspection was conducted by two trained raters, who independently annotated segments with visible blinks or muscular artifacts [54].

The experimental dataset consists of 3.864 EEG samples acquired from 23 subjects during controlled stress-induction tasks. Each sample corresponds to a fixed-length EEG segment processed using the proposed STCD feature extraction framework.

D. Feature Extraction Framework: Spatial–Temporal Connectivity Descriptor Framework (STCD)

Each segment is processed through two parallel branches: (i) a temporal branch, which extracts handcrafted statistical features from individual EEG channels, and (ii) a spatial branch, which encodes inter-channel relationships across electrode pairs, as shown in Table 1. These features are subsequently concatenated to form a unified representation suitable for classification.

In the temporal branch, time-domain descriptors are derived from each EEG channel to capture intra-signal morphology. The extracted features include mean, standard deviation, skewness, and kurtosis as well as Hjorth parameters: activity, mobility, and complexity [55]-[56]. Hjorth parameters provide a compact quantification of signal dynamics and have been widely used to characterize stress-induced neural modulation due to their physiological interpretability [57].

The spatial branch focuses on inter-channel interactions, computed across all possible electrode pairs. We incorporate three connectivity descriptors: (1) Pearson correlation is employed to quantify linear inter-channel dependencies between EEG signals, providing a compact representation of functional connectivity patterns among EEG channels [58]-[59]; (2) Amplitude asymmetry is used to capture hemispheric imbalance in EEG activity, which has been associated with stress-related neural responses [11];[21]; and (3) The Phase Lag Index (PLI) is adopted to estimate phase-based functional connectivity while reducing the Influence of volume conduction effects [60]-[61].

To capture nonlinear interactions between features, we introduced a meta-correlation descriptor defined as the Pearson correlation between the raw feature vector and its log-transformed version: Corr (f_{TS}, log (1 + $|f_{TS}|$))[18]. This transformation emphasizes relative changes in small-magnitude components while dampening extreme values, improving sensitivity to second-order relationships. Prior work in neuroimaging and bioinformatics supports the use of log-scaling to uncover latent structure in noisy physiological signals [62].

TABLE I. MATHEMATICAL FORMULATIONS AND VARIABLE DEFINITIONS FOR EACH DOMAIN-SPECIFIC FEATURE SET INCLUDED IN THE STCD FRAMEWORK

Domain	Formula	Variable Meaning
Temporal	$\mu = \frac{1}{N}\sum x_i, \sigma = \sqrt{\frac{1}{N}\sum (x_i - \mu)^2}$	x_i : EEG sample, N: Number of samples
	$A = Var(x), M = \sqrt{\frac{Var(x')}{Var(x)}}, C = \frac{M'}{M}$	A: Hjorth Activity, M: Mobility, C: Complexity
Spatial	$PLI = \langle sign(\sin(\emptyset_x - \emptyset_y))\rangle$	Phase Lag Index between signal phases $\emptyset_x$, $\emptyset_y$
	$\Delta_{ab} = \mu_a - \mu_b$	μ_a, μ_b : mean amplitude of channels a,b
Corr	$corr(x\_a, x\_b) = Cov(x\_a, x\_b) / (\sigma\_(x\_a).\sigma\_(x\_b))$	$Cov(x\_a, x\_b)$: the covariance between x_a, x_b and $\sigma\_(x\_a).\sigma\_(x\_b)$

		are their respective standard deviations. x : extracted feature
Meta-Corr	$Corr\_log\ (x\_a, x\_b\ ) = Corr(\log\ (1 + \lvert x\_a\ \rvert), \log\ (1 + \lvert x\_b\ \rvert))$	Correlation between original and log-transformed feature vector

The extracted features are subsequently classified using several machine learning algorithms, including XGBoost, SVM, Random Forest, KNN, Decision Tree, AdaBoost, and Naïve Bayes, under both binary and multiclass classification settings. Prior to classification, the feature matrix is standardized using z-score normalization (StandardScaler) [58]-[59].

E. Classification Strategy

The STCD framework integrates a broad range of classical machine learning algorithms, selected for their accuracy, interpretability, and computational efficiency, among other factors. For benchmarking the performance, eight machine learning classifiers are applied: XGBoost, Random Forest (RF), Support Vector Machine (SVM), k-Nearest Neighbors (KNN), Decision Tree (DT), AdaBoost, Gradient Boosting (GB), and Gaussian Naive Bayes (GNB) [63]. These models include ensemble methods, probabilistic models, distance-based classification, and kernel-based learning, allowing for a thorough evaluation of the proposed feature set [64].

XGBoost is chosen for its ability to handle complex decision boundaries via boosted trees and regularization [65], [66]. Random Forest builds multiple decision trees using different feature subsets, which increases the model's resistance to overfitting and noise [67]-[68]. Kernel-based models (SVM) can deliver a high discriminative power in complex feature spaces [69]-[70]. Instance-based models (KNN) are very effective with low-dimensional, handcrafted features [71]-[72]. AdaBoost and Gradient Boosting continuously improve the model by focusing on misclassifications [73]-[74]. Simple models (Naive Bayes, Decision Tree) can still offer computational benefits [75]-[76].

All the classifiers were trained on feature vectors extracted from hand-crafted descriptors. Hyperparameter tuning is performed using grid search within a cross-validation framework to ensure fair and consistent model optimization [77]-[78].

III. EVALUATION AND TESTING SCENARIO

The DASPS dataset included 23 participants, each completing 12 trials, yielding more than 3000 EEG segments after windowing. The segments were marked according to the valence-arousal (V-A) model for both the binary and four-class situations. The distribution of classes across binary and multiclass labels was nearly equal due to the stratified segmentation approach. Moreover, the counts of classes were checked to rule out overrepresentation bias, thus guaranteeing equal training and assessment.

In the binary setup, EEG segments received the label "Stress" when valence (V) was less than or equal to 5 and arousal (A) was greater than or equal to 5; otherwise, the label "No-Stress" was assigned. In the multiclass case, the labelling criteria for stress was further subdivided into three levels based on more specific V-A thresholds: Label 3 (v ∈ (0,2], a ∈ [7,9]), Label 2 (v ∈ (2,4], a ∈ [6,7)), and Label 1 (v ∈ (4,5], a ∈ [5,6)). Segments that did not satisfy these thresholds were assigned Label 0 as the default class. This granularity allows us to explore the more subtle levels of stress intensity in the EEG signals.

The total number of 462 features generated in the proposed scheme is summarized in Table 2. These features comprise 98 temporal descriptors and 364 spatial connectivity features. The temporal features are derived from the extraction of seven statistical and Hjorth-based descriptors from each of the 14 EEG channels. This gives a total of 7×14 = 98 features. The set of spatial features is created by applying four complementary measures of connectivity (Pearson correlation, amplitude asymmetry, Phase Lag Index (PLI), and log-transformed meta-correlation) across all unique pairs of EEG channels (14×13/2=91), yielding 4×91=364 spatial descriptors. The explicit quantification done here highlights the feature space that is structured but also high-dimensional, which gives an apparent reason to use classical machine learning classifiers.

TABLE II. FEATURE DIMENSIONALITY OF THE STCD FRAMEWORK

Feature Group	Description	Dimension
Temporal Features	Statistical and Hjorth parameters extracted per EEG channel (7 features × 14 channels)	98
Pearson Correlation	Pairwise correlation between temporal feature vectors across unique EEG channel pairs (14×13/2)	91
Amplitude Asymmetry	Mean amplitude difference between unique EEG channel pairs (14×13/2)	91
Phase Lag Index (PLI)	Phase-based connectivity measure computed for unique EEG channel pairs (14×13/2)	91
Meta-Correlation (Log)	Log-transformed correlation between temporal feature vectors of unique EEG channel pairs (14×13/2)	91

The stratified 5-fold cross-validation scheme was used to ensure the same class distribution across the training and evaluation pipelines, thereby achieving consistent results [79]. Eight different AI classifiers were trained and tested: the XGBoost, Random Forest, SVM, KNN, Decision Tree, AdaBoost, Gradient Boosting, and Gaussian Naive Bayes.

To avoid data leakage, hyperparameter tuning was performed using cross-validation. The hyperparameter optimization was performed globally within each cross-validation fold and was not influenced by subject-specific factors. This setup guarantees that model evaluation and generalization will be unbiased [80], as illustrated in Table 3.

TABLE III. HYPERPARAMETER SEARCH SPACE FOR MACHINE LEARNING CLASSIFIERS

Model	Parameter Configuration
XGB	n_estimators=[500, 1000, 1500, 2000], eval_metric='logloss', random_state=42

RF	n_estimators=[200, 500], max_depth=[10, None], random_state=42
SVM	kernel='rbf', probability=True, C=[1000, ..., 1e6], gamma='scale', random_state=42
KNN	n_neighbors=[3, 7, 13, 29, 57, 87, 135]
DT	criterion=['gini', 'entropy'], max_depth=range(3,15), random_state=42
AB	n_estimators=[50,100,200],learning_rate=[0.01,0.05,0.1,0.5,1.0], algorithm=['SAMME','SAMME.R'], random_state=42
GB	loss='log_loss', learning_rate=0.05 or 0.1, min_samples_split=2 or 5, min_samples_leaf=1 or 2, max_depth=3 or 5, max_features='sqrt', criterion='friedman_mse', subsample=0.8 or 1.0, n_estimators=100 or 200, random_state=42
NB	Default

IV. RESULT AND DISCUSSION

A. Binary Classification Performance

Overall, the classifiers demonstrated superior performance in the binary stress classification task. KNN achieved the highest accuracy (99.18% ± 0.28%) and F1-score (98.89% ± 0.38%), while SVM yielded the highest AUC (99.92% ± 0.02%) at the expense of substantial computational cost. XGBoost provided a favorable balance between classification accuracy (92.78%) and inference latency (0.0015s), supporting its suitability for real-time applications.

The K-Nearest Neighbors (KNN) classifier achieved the highest accuracy (99.18% ± 0.28%) and F1-score (98.89% ± 0.38%) in the binary stress classification task, along with a robust AUC of 99.89% ± 0.06%. It also maintained a relatively low training time (0.8828s) and acceptable inference latency (0.1271s), making it a practical choice for real-time stress monitoring. Support Vector Machine (SVM) also demonstrated excellent performance, achieving 98.93% accuracy and 98.55% F1-score, with an AUC of 99.92% ± 0.02%. However, it incurred the highest computational burden, with a training time of over 364 seconds and the highest inference time (3.5953s ± 0.2058s), limiting its suitability for latency-sensitive applications.

XGBoost (XGB) achieved the highest accuracy (92.78%) while maintaining extremely low inference time (0.0015s), making it well-suited for settings with limited resources. On the other hand, Random Forest (RF) showed low recall (70.87%) and F1-score (73.98%), though it had a good AUC of 98.85%, indicating that the model is sensitive to class imbalance in the binary stress context.

Simpler models such as Decision Tree (DT), AdaBoost (AB), and Gradient Boosting (GB) achieved moderate classification performance, with accuracies ranging from 75% to 81%, but suffered from lower recall and F1 Scores. While Gaussian Naive Bayes performed poorly in terms of accuracy and AUC, its low inference time (<0.01s) and minimal resource consumption suggest potential use in low-power or wearable platforms where interpretability and speed outweigh predictive precision, as shown in Table 4.

TABLE IV PERFORMANCE COMPARISON OF MACHINE LEARNING CLASSIFIERS FOR BINARY EEG-BASED STRESS CLASSIFICATION USING THE STCD FRAMEWORK

Model	Acc (%)	Re-call (%)	F1 Score (%)	AUC (%)	Training Time (s)	Inference Time (s)
XGB	92.78 ± 1.50	86.15 ± 2.95	89.29 ± 2.44	98.27 ± 0.61	23.0625 ± 0.7342	0.0015 ± 0.0003
SVM	98.93 ± 0.24	97.98 ± 0.45	98.55 ± 0.34	99.92 ± 0.02	364.542 ± 2.5534	3.5953 ± 0.2058
RF	85.64 ± 4.03	70.87 ± 8.18	73.98 ± 10.99	98.85 ± 1.62	112.4705 ± 4.1406	0.0502 ± 0.0039
KNN	99.18 ± 0.28	98.82 ± 0.51	98.89 ± 0.38	99.89 ± 0.06	0.8828 ± 0.0244	0.1271 ± 0.0169
DT	77.70 ± 0.42	57.13 ± 1.11	56.74 ± 1.83	69.49 ± 1.83	4.2994 ± 0.0221	0.0011 ± 0.0001
AB	75.79 ± 0.31	51.33 ± 0.70	46.01 ± 1.44	72.94 ± 1.48	79.9476 ± 0.1866	0.0449 ± 0.0016
GB	81.41 ± 0.71	62.71 ± 1.53	64.76 ± 2.14	90.01 ± 0.67	191.6342 ± 0.8847	0.0032 ± 0.0001
NB	49.90 ± 0.95	59.38 ± 0.77	49.23 ± 0.87	64.10 ± 0.75	0.2320 ± 0.0042	0.0065 ± 0.0007

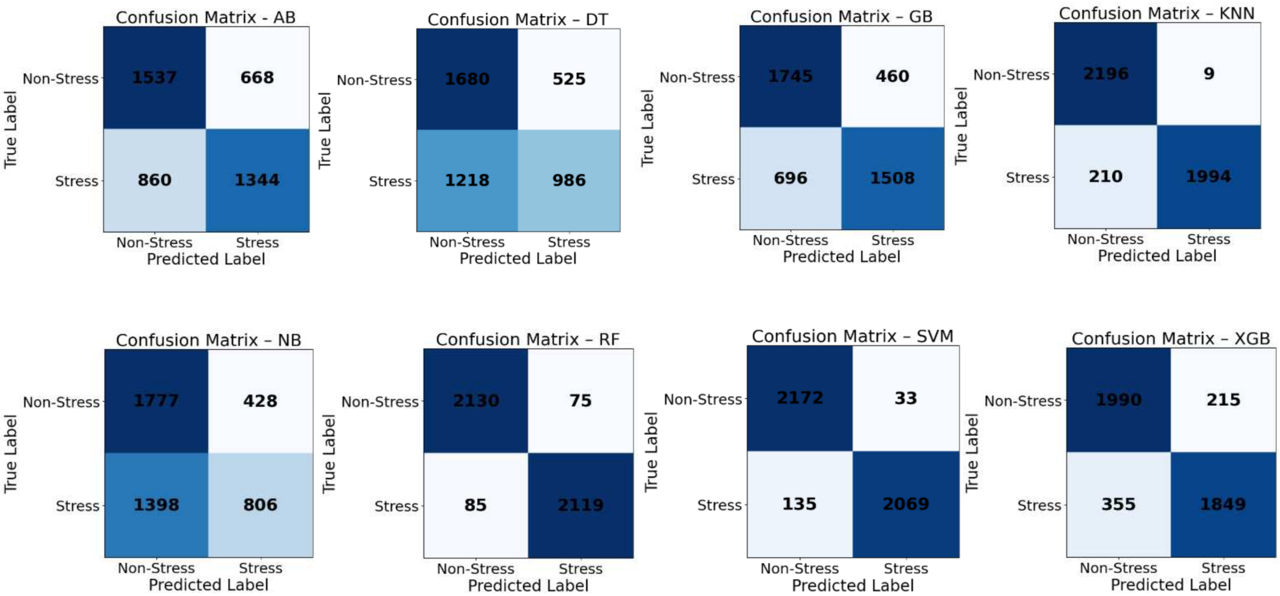

Fig. 5. Confusion matrices for binary stress classification (stress vs. non-stress)

Further analysis of class-wise performance and confusion matrices for the binary stress classification task is presented in Fig. 5. The results indicate consistently high negative rates for the non-stress class and intense sensitivity to stress, particularly for KNN and Random Forest, which exhibit the most balanced error distributions. In contrast, simpler models such as Decision Trees and Naïve Bayes show higher stress misclassification rates.

Validation of class separability is shown in Fig. 6 using Linear Discriminant Analysis (LDA). The LDA projection is presented solely for qualitative visualization purposes and does not serve as a quantitative validation of class separability or classifier performance. The 2D projection illustrates a clear margin between Class 0 (No-Stress) and Class 1 (Stress), forming two well-separated clusters along the first discriminant axis. The high classification scores, supported by the above visual evidence, and the ability of the handcrafted features to provide the relevant neural distinctions associated with stress states are thus highlighted.

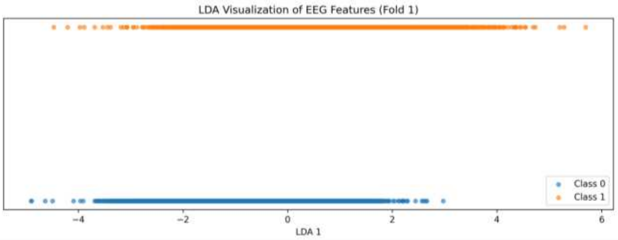

Fig. 6 Linear Discriminant Analysis (LDA) Visualization of Feature Space for Binary EEG Stress Classification Using Handcrafted STCD Features

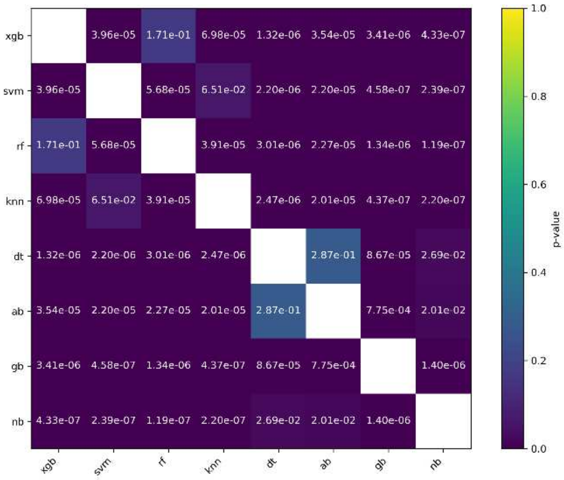

Fig. 7. Heatmap of paired t-test p-values for binary stress classification across classifiers

A matrix of paired t-test p-values for the binary classification task is shown in Fig. 7. The values of the matrix are less than 0.05. This indicates that there is a statistically significant difference in the performance of the compared classifiers. The high-performing models were particularly KNN, SVM, Random Forest, and XGBoost, and their performance gains were statistically significant compared with simpler classifiers such as Decision Tree, Naïve Bayes, and AdaBoost. Thus, it confirms that the improvements observed are not due to random variation.

B. Binary Model Efficiency Analysis

The training and estimation periods of each classifier were measured to assess their computational efficiency, a crucial factor for real-time EEG-based stress monitoring systems. Support Vector Machine (SVM) came to this conclusion due to its kernel-based optimization and difficulty in dealing with high-dimensional feature spaces, which resulted in the longest average training time of 364.54s ± 2.55s, as illustrated in Fig. 8 and Fig. 9. The next in line was Random Forest (RF) with a significant training time of 112.47s ± 4.14s, which was due to the extra time taken while making many random decision trees.

On the other hand, the simpler models, Naive Bayes (NB) and K-Nearest Neighbors (KNN), showed only very slight training times of 0.23s ± 0.0042s and 0.88s ± 0.02s, respectively. Their low model complexity and minimal or no parameter tuning were the reasons for this. XGBoost (XGB) and AdaBoost (AB) required moderate training times of 23.06s ± 0.73s and 79.95s ± 0.19s, respectively, while Gradient Boosting (GB) training time was the longest at 191.63s ± 0.88s, due to iterative optimization.

As for inference performance, SVM had the longest interval time at 3.5953s ± 0.2058s, making it the lowest in this regard among the classifiers, suitable for applications that require quick responses. KNN took longer due to its instance-based nature, at 0.1271s ± 0.0169s, while RF and AB were next, with moderate inference times of 0.0502s and 0.0449s, respectively. On the other hand, XGB and GB made the least noise, with remarkable inference delays of only 0.0015s and 0.0032s, respectively, making them quite the perfect candidates for real-time stress detection.

The quickest inference times were recorded by Decision Tree (DT) and Naive Bayes (NB), with average times of 0.0011s and 0.0065s, respectively. Nonetheless, these models sacrifice their speed for the lower classification accuracy. All in all, XGB has the strongest classifier, meeting the low computational requirements while providing excellent predictive performance.

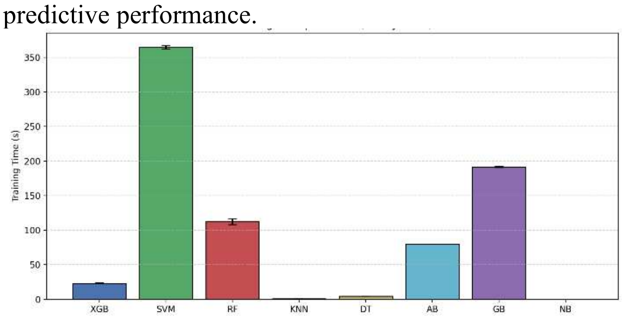

Fig. 8. Comparison of training time across different machine learning classifiers in binary EEG stress classification using the proposed STCD.

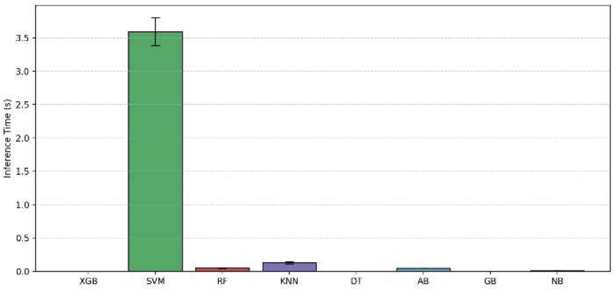

Fig. 9. Comparison of inference time across different machine learning classifiers in binary EEG stress classification using the proposed STCD.

C. Multiclass Classification Performance

The same performance pattern can be seen in the multiclass classification setting as well. KNN and SVM were the top performers in classification accuracy (98.73% ± 0.23%) and AUC (99.86% ± 0.05%) throughout the study, while XGBoost delivered strong results at a much lower cost in inference latency (0.0062s ± 0.0011s). On the other hand, the less complex classifiers proved to be less accurate despite their computational efficiency.

TABLE V PERFORMANCE COMPARISON OF MACHINE LEARNING CLASSIFIERS FOR MULTICLASS EEG-BASED STRESS CLASSIFICATION USING THE STCD FRAMEWORK

Model	Acc (%)	Re-call (%)	F1 Score (%)	AUC (%)	Training Time (s)	Inference Time (s)
XGB	93.77 ± 0.38	89.65 ± 1.21	92.82 ± 0.77	99.54 ± 0.04	91.5989 ± 1.1878	0.0062 ± 0.0011
SVM	98.56 ± 0.33	97.10 ± 0.40	98.09 ± 0.33	99.95 ± 0.03	394.0696 ± 3.3347	4.9516 ± 0.1316
RF	88.99 ± 0.46	76.01 ± 1.17	83.08 ± 0.93	99.84 ± 0.03	141.2018 ± 24.9999	0.1011 ± 0.0387
KNN	98.73 ± 0.23	98.13 ± 0.45	98.44 ± 0.18	99.86 ± 0.05	0.8881 ± 0.0176	0.1379 ± 0.0164
DT	63.18 ± 1.40	40.70 ± 5.01	44.01 ± 6.40	70.91 ± 3.19	4.0353 ± 0.2369	0.0012 ± 0.0000
AB	56.29 ± 0.94	31.30 ± 0.72	31.50 ± 1.42	69.62 ± 1.18	72.0877 ± 9.5432	0.0438 ± 0.0148
GB	78.71 ± 0.55	64.61 ± 0.81	71.91 ± 0.78	94.02 ± 0.26	765.3867 ± 0.8916	0.0089 ± 0.0001
NB	49.86 ± 0.51	46.27 ± 0.81	35.69 ± 0.73	69.08 ± 0.41	0.6430 ± 0.0128	0.0105 0.0006

According to Table 5, the K-Nearest Neighbors (KNN) classifier is the winner among all classifiers for multiclass mental stress classification, with an accuracy of 98.73% ± 0.23%, an F1-score of 98.44% ± 0.18%, and an AUC of 99.86% ± 0.05%. This performance confirms that KNN has strong generalization and differentiation abilities across different stress levels. The Support Vector Machine (SVM) ranks second, with slightly lower accuracy (98.56% ± 0.33%) but the highest AUC (99.95% ± 0.03%), indicating its stability despite the high computational resource requirements.

XGBoost (XGB) provided a compromise in performance, achieving 93.77% ± 0.38% accuracy and 92.82% ± 0.77% F1-score, along with very short inference latency (0.0062s ± 0.0011s), further confirming its usefulness in real-time settings. Unexpectedly, Random Forest (RF), though having a considerable AUC (99.84% ± 0.03%), ended up with poorer classification metrics (accuracy: 88.99%, F1-score: 83.08%) and also showed inconsistency in recall performance (76.01% ± 1.17%), which could be a result of overfitting or being too susceptible to the class imbalance.

At the bottom of the scale, Decision Tree (DT), AdaBoost (AB), and Naive Bayes (NB) were far behind the others in performance. DT and AB had F1-scores lower than 45%, while NB had the worst precision (F1: 35.69%) even though it was the fastest to train (0.6430s ± 0.0128s) and had a relatively low inference time (0.0105s ± 0.0006s). On the other hand, Gradient Boosting (GB) was the slowest during training (765.39s ± 0.89s) and achieved only moderate performance (accuracy: 78.71%, F1-score: 71.91%), making it less suitable for efficiency-constrained situations.

In terms of inference time, SVM again posed challenges for real-time applications due to its high latency (4.9516s ± 0.13s). At the same time, KNN (0.1379s) and RF (0.1011s) required moderate prediction times due to their instance-based and ensemble complexities, respectively.

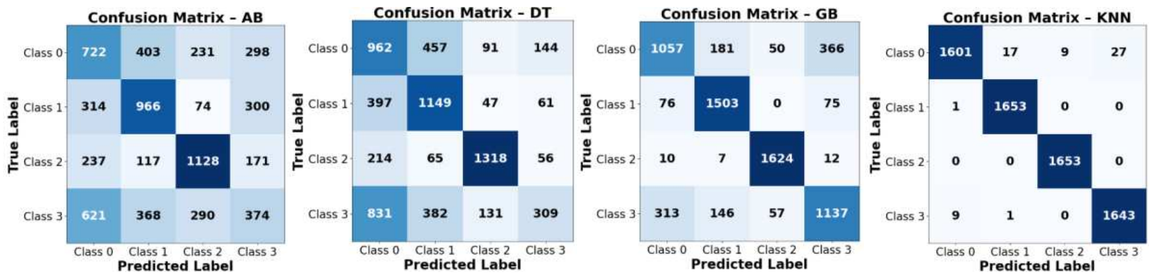

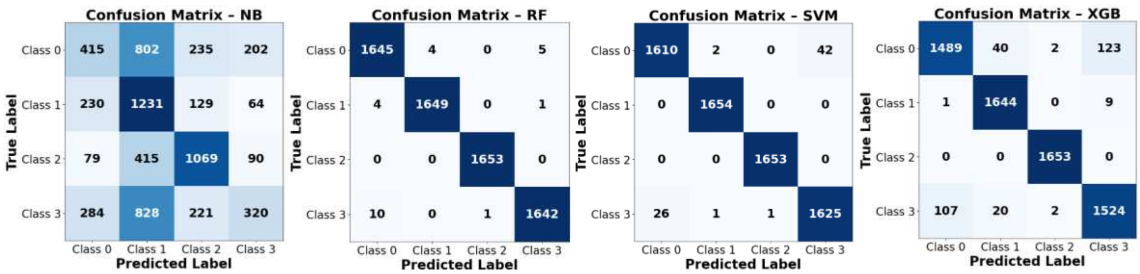

Fig. 10. Confusion matrices for multiclass stress classification

Figure 10 depicts the confusion matrices of the four-class stress classification. KNN, Random Forest, SVM, and XGBoost exhibit excellent class-wise discrimination, as evidenced by high diagonal dominance, indicating correct identification across all levels of stress. On the other hand, the Decision Tree and the Naïve Bayes classifiers exhibit significant blending of adjacent classes, particularly at intermediate stress levels. This reflects the difficulty in separating the subtle neurophysiological transitions.

The distribution of features was qualitatively assessed using Linear Discriminant Analysis (LDA), as illustrated in Fig. 11, solely for visualization and not for performance validation. The four classes generally appear as well-separated clusters, with Class 2 being the most distinct, while slight overlaps exist between the neighboring classes. In general, the visualization suggests that the features extracted by STCD remain highly separable across classes in the multi-class scenario.

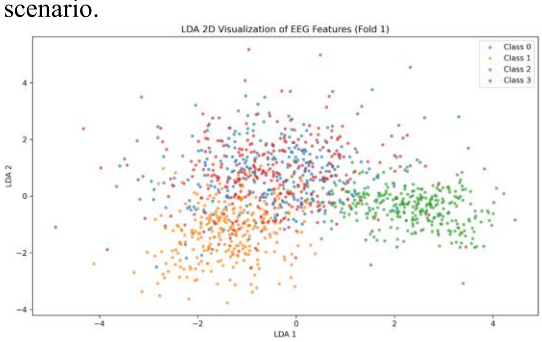

Fig. 11. LDA Visualization of Feature Space for Multiclass EEG Stress Classification Using Handcrafted STCD Features

In Fig. 12, the matrix of p-values from the paired t-test for multiclass stress classification through different classifiers is shown. Statistically significant performance differences are indicated by values below the 0.05 threshold, suggesting that the observed accuracy differences are not due to random variation. The findings reveal that the models with the best performance, especially KNN, SVM, Random Forest, and XGBoost, have considerable statistical superiority over the simpler classifiers, namely, Decision Tree, AdaBoost, and Naïve Bayes, thus proving their multiclass classification performance to be robust.

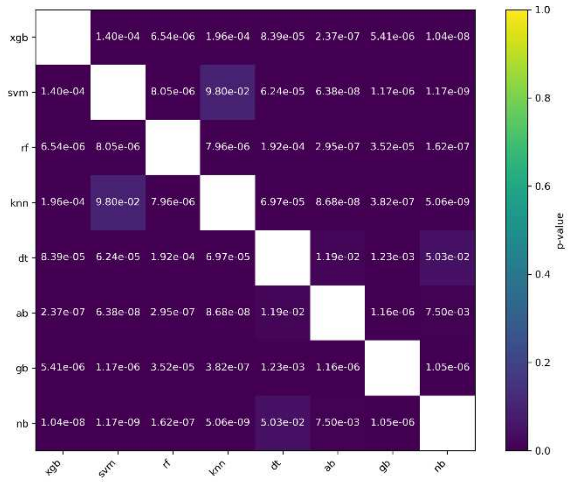

Fig. 12. Heatmap of paired t-test p-values for multiclass stress classification across classifiers

D. Multiclass Model Efficiency Analysis

We also assessed the time required for STCD framework training and the inference time of its classifiers to measure its computational efficiency in the multiclass problem scenario, as depicted in Figs. 13 and 14. Gradient Boosting (GB) required the longest training time (765.39s ± 0.89s), followed by Support Vector Machine (SVM) and Random Forest (RF), with training times of 394.07s ± 3.33s and 141.20s ± 25.00s, respectively. The lengthy training time was due to the initial stage of training in GB and to the computationally intensive kernel methods in RF and SVM.

On the other hand, K-Nearest Neighbors (KNN) and Naive Bayes (NB) were the fastest to train, with 0.8881s ± 0.0176s and 0.6430s ± 0.0128s, respectively, further highlighting their computational simplicity. Decision Tree (DT) likewise had a quick training time of 4.0353s ± 0.2369s, but AdaBoost (AB) and XGBoost (XGB) kept the training durations average.

SVM is again the slowest classifier, with a latency of 4.9516s ± 0.1316s, making it unsuitable for real-time EEG classification. RF and KNN provided moderate inference times of 0.1011s and 0.1379s, respectively, which reflect the cost of multiple tree evaluations or distance calculations. Meanwhile, Decision Tree (0.0012s) and XGBoost (0.0062s) produced very fast predictions, making them suitable for the applications. Naive Bayes also maintained low latency (0.0105s), further emphasizing its lightweight computational profile despite lower classification accuracy.

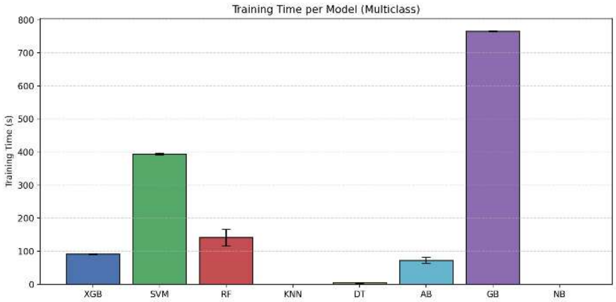

Fig. 13 Comparison of training time across different machine learning classifiers in multiclass EEG stress classification using the proposed STCD feature set

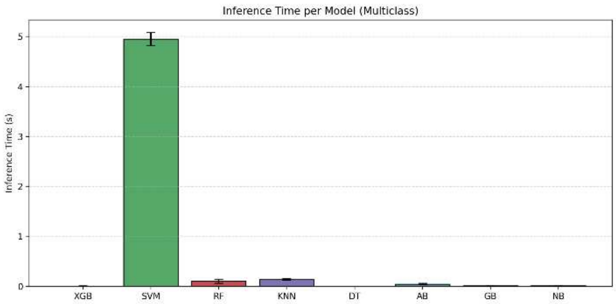

Fig. 14 Comparison of inference time across different machine learning classifiers in multiclass EEG stress classification using the proposed STCD feature set

Table 6 presents the optimal hyperparameter configurations for each classifier, determined through grid search within a stratified 5-fold cross-validation. These configurations represent the optimal parameter settings for maximizing classification performance with the proposed handcrafted EEG feature set.

TABLE VI. THE OPTIMAL HYPERPARAMETERS FOR EACH CLASSIFIER USING STRATIFIED 5-FOLD CROSS-VALIDATION

Classifier	Optimal Hyperparameter
SVM	C=10000, kernel=rbf
RF	n_estimators=500, max_depth=None, criterion=gini
KNN	n_neighbors=3
DT	max_depth=6, criterion=gini
AB	n_estimators=100, learning_rate=1.0, algorithm=SAMME
GB	n_estimators=100, learning_rate=0.1, loss=log_loss
NB	(No tunable hyperparameters)
XGB	n_estimators=1000, learning_rate=0.1, max_depth=3

Table 7 provides a contextual comparison between the proposed framework and representative prior studies on EEG-based stress classification. While direct numerical comparison across heterogeneous protocols should be interpreted with caution, the results indicate that the proposed approach achieves competitive performance within the DASPS experimental setting. As summarized, prior studies primarily employed temporal–frequency features (83.5%, 74.6%) [54], statistical spatial–temporal descriptors without explicit connectivity modeling (83.8%) [52], or data-level augmentation strategies such as S-LSMOTE (89.5%) [55]. None of these works explicitly integrated connectivity-based descriptors or reported latency analysis of inference. In contrast, the proposed framework incorporates interpretable spatial connectivity descriptors at the feature level. It evaluates both classification performance and computational efficiency, achieving 99.18% accuracy for binary (KNN) and 98.56% for multiclass (SVM).

TABLE VII. PERFORMANCE COMPARISON TABLE

Approach	Methods	Classification	Classifier	Acc (%)
Baghdadi et al[49]	TFF	Binary	Auto encoder	83.5
Baghdadi et al[49]	TFF	Multiclass	Auto encoder	74.6
Chatterje[47]	STT	Binary	K-NN	83.8
Chatterje [47]	STT	Multiclass	K-NN	83.8
Syakiyla et al[50]	S-LSMOTE	Multiclass	K-NN	89.5
Proposed	STCD	Binary	KNN	99.18
Proposed	STCD	Multiclass	SVM	98.56

E. Discussion

The present study illustrates that the proposed handcrafted Spatial–Temporal Connectivity Descriptor (STCD) framework is very efficient for EEG-based mental stress recognition in both binary and multiclass classification. The experimental results consistently show that the extracted spatial–temporal connectivity features enable intense discrimination between stress levels, as evidenced by high accuracy, AUC, and F1-score across multiple classical machine learning classifiers. Macro-averaged F1-score is used as the primary per-class performance indicator. In particular, KNN and SVM achieved the highest classification performance, while XGBoost exhibited an optimal balance between predictive accuracy and computational efficiency. The confusion matrix analysis further confirms stable class-wise prediction behavior, indicating that the reported performance is not driven by class imbalance but reflects robust feature separability.

Compared with representative prior studies on EEG-based stress detection, including the proposed STCD framework achieves competitive and, in several cases, superior classification performance within the DASPS experimental setting [47], [49], [50]. While earlier approaches relied on temporal-frequency features, data-level balancing, or deep autoencoder-based representations, the present work emphasizes interpretable handcrafted spatial–temporal connectivity descriptors combined with classical classifiers. It should be noted that direct numerical comparison across studies must be interpreted with caution due to differences in datasets, segmentation strategies, and validation protocols. Nevertheless, under a consistent evaluation framework, the results indicate that systematically integrating spatial connectivity measures with temporal descriptors provides a meaningful advantage for stress recognition.

The strong performance of the STCD framework can be attributed to its ability to capture complementary neurophysiological information. Temporal descriptors characterize local signal dynamics, while spatial connectivity measures, such as Pearson correlation, amplitude asymmetry, and the Phase Lag Index, encode inter-channel interactions associated with stress-related neural synchronization. The inclusion of a log-transformed meta-correlation descriptor further stabilizes feature distributions and enhances robustness against variability. From a modeling perspective, instance-based and margin-based classifiers, particularly KNN and SVM, benefit from the structured and discriminative nature of the handcrafted feature space. In contrast, tree-based ensemble models offer improved robustness at the expense of higher training cost, while simpler classifiers trade predictive accuracy for computational efficiency.

Interpretability, modularity, and computational efficiency are the main advantages of the STCD framework proposed in this study. The method remains transparent and suitable for real-time or resource-limited EEG applications by avoiding complex deep learning architectures. However, there are still a few limitations to consider. The single publicly available dataset was used for evaluation, and the experimental setup was offline; hence, there was no subject-independent or out-of-distribution validation. Moreover, EEG signals are sensitive to artifacts and inter-subject variability, which can lead to reduced generalization during real-world deployment. These limitations motivate future investigations into robustness analysis, subject-independent evaluation schemes, and real-time implementation on wearable EEG platforms.

F. Summary of Key Findings and Practical Implications

To facilitate more straightforward interpretation of the experimental results, the key findings from both binary and multiclass stress classification tasks are summarized as follows:

- KNN and SVM achieved the highest classification accuracy and AUC across both binary and multiclass settings, demonstrating the strong discriminative capability of the proposed STCD features.
- XGBoost consistently provided an optimal trade-off between predictive performance and inference efficiency, making it the most suitable candidate for real-time EEG-based stress monitoring systems.
- ree-based ensemble models exhibited robust performance but incurred higher training costs, potentially limiting scalability in resource-constrained environments.
- Simpler models like Naive Bayes and Decision Trees were less computationally intensive but had much lower classification accuracy, suggesting a trade-off between efficiency and predictive precision.

V. CONCLUSION

In this paper, we propose an EEG-based mental stress recognition framework that is interpretable and modular, based on a handcrafted Spatial-Temporal Connectivity Descriptor (STCD). Theoretically, the described method combines the varieties of time- and space-connectedness into a single feature representation, which is probably the only such case among stress EEG analysis techniques as an alternative to the deep fusion architectures widely used today.

First, the STCD framework demonstrated strong discriminative power in classifying stress across binary and multiclass categories. KNN was the top classifier in both cases; meanwhile, XGBoost was consistently the best for a balance of accuracy and performance speed. On the other hand, SVM achieved high accuracy, but its high reference latency made it less appropriate for applications requiring a quick response [81].

Second, the performance evaluation of eight classic classifiers confirmed that KNN and XGBoost are the fastest models suitable for real-time applications, offering the best trade-off between accuracy and computational cost [86]. While SVM was entirely accurate, it was also impossible to train and perform inference due to the significant time required [82].

Third, the new method beats competitors in the DASPS experimental conditions, showing the power of artisanal spatiotemporal connectivity descriptors under uniform evaluation protocols. These advantages demonstrate the robustness and representational strength of the STCD descriptors in accurately covering EEG dynamics related to stress, whether the dataset is balanced or not. This contrasts with recent EEG-based stress recognition studies that have used deep or hybrid architectures.

These results point out that the examination of binary and multiclass stress settings systematically combining spatiotemporal EEG features and descriptors of spatial connectivity in an integrated way, this work provides a new leading that meticulously crafted representations can be on par with the existing ones in terms of performance, and at the same time, be easy to interpret and inexpensive to compute; thus, they are especially appropriate for real-world applications, such as, among others, wearable mental health monitoring devices, workplace stress assessment systems, and adaptive human–computer interaction platforms where transparency and computational efficiency are of utmost importance. This suggests that connectivity-driven EEG features can be used without the need for deep or hybrid architectures in the current scenario.

Despite these positive aspects, it is worth noting some drawbacks. The Research was carried out on a single publicly available dataset (DASPS), which may impose limitations on dataset size, demographic makeup, and the experimental protocol. The proposed framework could only be evaluated in an offline setting, and longitudinal or out-of-lab validation was not conducted; hence, the results might not be highly generalizable to real-world conditions. Also, EEG signals were subjected to standard preprocessing. However, artifacts and inter-subject variability remain the main factors affecting EEG signals, which can lower classification accuracy in practical scenarios.

As a result, the future direction for the Modified Detection System will be in line with the existing system, aiming to preserve its handcrafted and easily interpretable design principles. Future Research will focus on feature weighting strategies using the system, robustness analysis under nonstationary EEG conditions, and leave-one-subject-out validation. Continued validation is needed.

REFERENCES

[1] G. Giannakakis, D. Grigoriadis, and M. Tsiknakis, "Detection of stress/anxiety state from EEG features during memory and arithmetic tasks using machine learning classifiers," *Brain Sci.*, vol. 12, no. 2, p. 240, 2022.

[2] P. Nie, K. Zhao, D. Ma, H. Liu, S. Amin, and I. Yasin, "Global Climate Change, Mental Health, and Socio-Economic Stressors: Toward Sustainable Interventions across Regions," *Sustainability*, vol. 16, no. 19, p. 8693, 2024.

[3] H. F. van der Molen, K. Nieuwenhuijsen, M. H. Frings-Dresen, and G. de Groene, "Work-related psychosocial risk factors for stress-related mental disorders: an updated systematic review and meta-analysis," *BMJ Open*, vol. 10, no. 7, p. e034849, 2020.

[4] A. F. Arnsten and T. Shanafelt, "Physician distress and burnout: the neurobiological perspective," in *Mayo Clinic Proceedings*, Elsevier, 2021, pp. 763–769.

[5] R. Walker *et al.*, "Connection to... addressing digital inequities in supporting the well-being of young Indigenous Australians in the wake of COVID-19," *Int. J. Environ. Res. Public. Health*, vol. 18, no. 4, p. 2141, 2021.

[6] H. Murad, "Cultural stress: The undiagnosed epidemic of our time," *J. Integr. Med.*, vol. 21, no. 3, pp. 221–225, 2023.

[7] M. U. Bokhari, G. Yadav, and M. Zeyauddin, "Innovating workplace mental health strategies with advanced machine learning: application of a superior ensemble classifier for accurate stress detection in business environments," *Int. J. Inf. Technol.*, pp. 1–16, 2024.

[8] R. K. Rai and D. K. Singh, "Stress detection through wearable EEG technology: A signal-based approach," *Comput. Electr. Eng.*, vol. 126, p. 110478, 2025.

[9] R. Sharma and H. K. Meena, "Emerging trends in EEG signal processing: A systematic review," *SN Comput. Sci.*, vol. 5, no. 4, p. 415, 2024.

[10] M. Razavi *et al.*, "Machine learning, deep learning, and data preprocessing techniques for detecting, predicting, and monitoring stress and stress-related mental disorders: scoping review," *JMIR Ment. Health*, vol. 11, p. e53714, 2024.

[11] Y. Badr, U. Tariq, F. Al-Shargie, F. Babiloni, F. Al Mughairbi, and H. Al-Nashash, "A review on evaluating mental stress by deep learning using EEG signals," *Neural Comput. Appl.*, vol. 36, no. 21, pp. 12629–12654, 2024.

[12] J. R. Homberg and J. Jagiellowicz, "A neural model of vulnerability and resilience to stress-related disorders linked to differential susceptibility," *Mol. Psychiatry*, vol. 27, no. 1, pp. 514–524, 2022.

[13] F. Ghasemi, D. Q. Beversdorf, and K. C. Herman, "Stress and stress responses: A narrative literature review from physiological mechanisms to intervention approaches," *J. Pac. Rim Psychol.*, vol. 18, p. 18344909241289222, 2024.

[14] S. A. M. Mane, "StressNet: Hybrid model of LSTM and CNN for stress detection from electroencephalogram signal (EEG)," *Results in Control and Optimization*, vol. 11. 2023.

[15] H. M. Afify, "Stress detection based EEG under varying cognitive tasks using convolution neural network," *Neural Computing and Applications*, vol. 37, no. 7. pp. 5381–5395, 2025.

[16] G. Vos, M. Ebrahimpour, L. van Eijk, Z. Sarnyai, and M. R. Azghadi, "Stress monitoring using Low-Cost electroencephalogram devices: a systematic literature review," *Int. J. Med. Inf.*, p. 105859, 2025.

[17] R. Tanwar, G. Singh, and P. K. Pal, "A hybrid transposed attention based deep learning model for wearable and explainable stress recognition," *Comput. Electr. Eng.*, vol. 119, p. 109551, 2024.

[18] S. Acharya, A. Khosravi, D. Creighton, R. Alizadehsani, and U. R. Acharya, "Neurostressology: A systematic review of EEG-based automated mental stress perspectives," *Inf. Fusion*, p. 103368, 2025.

[19] M. M. H. Shuvo, S. K. Islam, J. Cheng, and B. I. Morshed, "Efficient acceleration of deep learning inference on resource-constrained edge devices: A review," *Proc. IEEE*, vol. 111, no. 1, pp. 42–91, 2022.

[20] A. Craik *et al.*, "Design and Validation of a Low-Cost Mobile EEG-Based Brain–Computer Interface," *Sensors*, vol. 23, no. 13, p. 5930, 2023.

[21] E. Gkintoni, A. Aroutzidis, H. Antonopoulou, and C. Halkiopoulos, "From neural networks to emotional networks: A systematic review of EEG-based emotion recognition in cognitive neuroscience and real-world applications," *Brain Sci.*, vol. 15, no. 3, p. 220, 2025.

[22] M. Bolpagni, S. Pardini, M. Dianti, and S. Gabrielli, "Personalized stress detection using biosignals from wearables: A scoping review," *Sensors*, vol. 24, no. 10, p. 3221, 2024.

[23] M. Kang, S. Shin, J. Jung, and Y. Kim, "Classification of Mental Stress Using CNN-LSTM Algorithms with Electrocardiogram Signals," *J. Healthc. Eng.*, vol. 2021, 2021.

[24] B. Chakravarthi, S.-C. Ng, M. Ezilarasan, and M.-F. Leung, "EEG-based emotion recognition using hybrid CNN and LSTM classification," *Front. Comput. Neurosci.*, vol. 16, p. 1019776, 2022.

[25] Z. Zhang, X. Ding, X. Liang, Y. Zhou, B. Qin, and T. Liu, "Brain and cognitive science inspired deep learning: a comprehensive survey," *IEEE Trans. Knowl. Data Eng.*, 2025.

[26] W. Ma, Y. Zheng, T. Li, Z. Li, Y. Li, and L. Wang, "A comprehensive review of deep learning in EEG-based emotion recognition: classifications, trends, and practical implications," *PeerJ Comput. Sci.*, vol. 10, p. e2065, 2024.

[27] S. Hana, R. Hassan, A. R. Faizabadi, A. Gubbi, M. Z. Bellary, and V. Manjula, "Enhanced EEGNet Optimization Using Lightweight Deep Neural Network for Detecting Human Stress Levels from Raw EEG Signals Dataset," in *2025 3rd International Conference on Integrated Circuits and Communication Systems (ICICACS)*, 2025, pp. 1--6.

[28] E. P. Torres, E. A. Torres, M. Hernández-Álvarez, and S. G. Yoo, "EEG-based BCI emotion recognition: A survey," *Sensors*, vol. 20, no. 18, p. 5083, 2020.

[29] E. Shi *et al.*, "Fome: A foundation model for eeg using adaptive temporal-lateral attention scaling," *ArXiv Prepr. ArXiv240912454*, 2024.

[30] A. Chaddad, Y. Wu, R. Kateb, and A. Bouridane, "Electroencephalography signal processing: A comprehensive review and analysis of methods and techniques," *Sensors*, vol. 23, no. 14, p. 6434, 2023.

[31] C. Avian *et al.*, "Temporal Spatial and Signal Descriptor Feature Extraction for Electronic Nose Signal Processing," *IEEE Sens. J.*, 2024.

[32] W. Guo, Y. Li, M. Liu, R. Ma, and Y. Wang, "Functional connectivity-enhanced feature-grouped attention network for cross-subject EEG emotion recognition," *Knowl.-Based Syst.*, vol. 283, p. 111199, 2024.

[33] L. Hu, C. Tan, J. Xu, R. Qiao, Y. Hu, and Y. Tian, "Decoding emotion with phase--amplitude fusion features of EEG functional connectivity network," *Neural Netw.*, vol. 172, p. 106148, 2024.

[34] M. Roshanaei, H. Norouzi, J. Onton, S. Makeig, and A. Mohammadi, "EEG-based functional and effective connectivity patterns during emotional episodes using graph theoretical analysis," *Sci. Rep.*, vol. 15, no. 1, p. 2174, 2025.

[35] W. Meng *et al.*, "Emotion recognition via affective EEG signals: State of the art," *Neurocomputing*, p. 130418, 2025.

[36] T. Li, B. Fu, Z. Wu, and Y. Liu, "Eeg-based emotion recognition using spatial-temporal-connective features via multi-scale CNN," *IEEE Access*, vol. 11, pp. 41859--41867, 2023.

[37] F. Hu *et al.*, "STRFLNet: Spatio-Temporal representation fusion learning network for EEG-Based emotion recognition," *IEEE Trans. Affect. Comput.*, 2025.

[38] S. Liu *et al.*, "Dynamic collaborative evolutionary network: A novel spatiotemporal feature extraction framework for EEG emotion recognition," *Expert Syst. Appl.*, p. 129654, 2025.

[39] X. Yang, Z. Zhu, G. Jiang, D. Wu, A. He, and J. Wang, "DC-ASTGCN: EEG emotion recognition based on fusion deep directional and adaptive spatio-temporal graph convolutional networks," *IEEE J. Biomed. Health Inform.*, 2024.

[40] A. Miljevic, O. W. Murphy, P. B. Fitzgerald, and N. W. Bailey, "Estimating sensor-space EEG connectivity PART 1: Identifying best performing methods for functional connectivity in simulated data," *Clin. Neurophysiol.*, vol. 174, pp. 73--83, 2025.

[41] L. Wei, T. Qiu, Z. Wang, and W. Mei, "A functional connectivity metric method for EEG time series via nonlinear symbolization," *Biomed. Signal Process. Control*, vol. 103, p. 107498, 2025.

[42] J. Xu, W. Qian, L. Hu, G. Liao, and Y. Tian, "EEG decoding for musical emotion with functional connectivity features," *Biomed. Signal Process. Control*, vol. 89, p. 105744, 2024.

[43] P. Samal and M. F. Hashmi, "Role of machine learning and deep learning techniques in EEG-based BCI emotion recognition system: a review," *Artif. Intell. Rev.*, vol. 57, no. 3, p. 50, 2024.

[44] L. Trujillo, D. E. Hernandez, A. Rodriguez, O. Monroy, and O. Villanueva, "Effects of feature reduction on emotion recognition using EEG signals and machine learning," *Expert Syst.*, vol. 41, no. 8, p. e13577, 2024.

[45] R. Sahu, S. R. Dash, L. A. Cacha, R. R. Poznanski, and S. Parida, "Epileptic seizure detection: a comparative study between deep and traditional machine learning techniques," *J. Integr. Neurosci.*, vol. 19, no. 1, pp. 1--9, 2020.

[46] F. Zheng, B. Hu, X. Zheng, and Y. Zhang, "Spatial–temporal features-based EEG emotion recognition using graph convolution network and long short-term memory," *Physiol. Meas.*, vol. 44, no. 6, p. 065002, 2023.

[47] D. Chatterjee, "Detection of mental stress using novel spatio-temporal distribution of brain activations," *Biomedical Signal Processing and Control*, vol. 82. 2023.

[48] M. Benchekroun, P. E. Velmovitsky, D. Istrate, V. Zalc, P. P. Morita, and D. Lenne, "Cross dataset analysis for generalizability of HRV-based stress detection models," *Sensors*, vol. 23, no. 4, p. 1807, 2023.

[49] A. Baghdadi, Y. Aribi, R. Fourati, N. Halouani, P. Siarry, and A. M. Alimi, "Dasps: A database for anxious states based on a psychological stimulation," *ArXiv Prepr. ArXiv190102942*, 2019.

[50] S. N. Syakiylla Sayed Daud, R. Sudirman, and T. Wee Shing, "Safe-level SMOTE method for handling the class imbalanced problem in electroencephalography dataset of adult anxious state," *Biomed. Signal Process. Control*, vol. 83, p. 104649, May 2023.

[51] S. Aburakhia, A. Shami, and G. K. Karagiannidis, "On the intersection of signal processing and machine learning: A use case-driven analysis approach," *ArXiv Prepr. ArXiv240317181*, 2024.

[52] I. Kiskin, D. Zilli, Y. Li, M. Sinka, K. Willis, and S. Roberts, "Bioacoustic detection with wavelet-conditioned convolutional neural networks," *Neural Comput. Appl.*, vol. 32, no. 4, pp. 915–927, 2020.

[53] M. K. Islam, A. Rastegarnia, and S. Sanei, "Signal artifacts and techniques for artifacts and noise removal," in *Signal Processing Techniques for Computational Health Informatics*, Springer, 2020, pp. 23–79.

[54] R. Ghosh, S. Phadikar, N. Deb, N. Sinha, P. Das, and E. Ghaderpour, "Automatic Eyeblink and Muscular Artifact Detection and Removal From EEG Signals Using k-Nearest Neighbor Classifier and Long Short-Term Memory Networks," *IEEE Sens. J.*, vol. 23, no. 5, pp. 5422–5436, Mar. 2023.

[55] M. S. Safi and S. M. M. Safi, "Early detection of Alzheimer's disease from EEG signals using Hjorth parameters," *Biomed. Signal Process. Control*, vol. 65, p. 102338, 2021.

[56] "Mental stress classification based on selected electroencephalography channels using correlation coefficient of hjorth parameters," *Brain Sci.*, vol. 13, no. 9, p. 1340, 2023.

[57] R. Fu, "Symmetric Convolutional and Adversarial Neural Network Enables Improved Mental Stress Classification From EEG," *IEEE Transactions on Neural Systems and Rehabilitation Engineering*, vol. 30. pp. 1384–1400, 2022.

[58] R. Dhiman and others, "Electroencephalogram channel selection based on pearson correlation coefficient for motor imagery-brain-computer interface," *Meas. Sens.*, vol. 25, p. 100616, 2023.

[59] D. Liu, Q. Ding, M. Wen, and C. Tong, "A Novel Generalized EEG Channel Selection Method Using Pearson Correlation Coefficient," in *2023 IEEE International Conference on Robotics and Biomimetics (ROBIO)*, 2023, pp. 1–6.

[60] F. Saffari, K. Norouzi, L. E. Bruni, S. Zarei, and T. Z. Ramsøy, "Impact of varying levels of mental stress on phase information of EEG Signals: A study on the Frontal, Central, and parietal regions," *Biomed. Signal Process. Control*, vol. 86, p. 105236, 2023.

[61] H. Kumar, N. Ganapathy, S. D. Puthankattil, and R. Swaminathan, "Analysis of EEG Fluctuation Patterns Using Nonlinear Phase-Based Functional Connectivity Measures for Emotion Recognition," *Fluct. Noise Lett.*, vol. 23, no. 05, p. 2450051, 2024.

[62] S. S. Nair, R. F. Kunz, W. Zhang, and X. I. Yang, "Rough-wall modeling on a low-dimensional manifold," *Phys. Rev. Fluids*, vol. 10, no. 6, p. 064606, 2025.

[63] S. Laghmati, S. Hamida, K. Hicham, B. Cherradi, and A. Tmiri, "An improved breast cancer disease prediction system using ML and PCA," *Multimed. Tools Appl.*, vol. 83, no. 11, pp. 33785–33821, 2024.

[64] S. Mallik and Z. Zhao, "Graph-and rule-based learning algorithms: a comprehensive review of their applications for cancer type classification and prognosis using genomic data," *Brief. Bioinform.*, vol. 21, no. 2, pp. 368–394, 2020.

[65] S. Demir and E. K. Sahin, "An investigation of feature selection methods for soil liquefaction prediction based on tree-based ensemble algorithms using AdaBoost, gradient boosting, and XGBoost," *Neural Comput. Appl.*, vol. 35, no. 4, pp. 3173–3190, 2023.

[66] H. Asemi and N. Farajzadeh, "Improving EEG signal-based emotion recognition using a hybrid GWO-XGBoost feature selection method," *Biomed. Signal Process. Control*, vol. 99, p. 106795, 2025.

[67] E. Halabaku and E. Bytyçi, "Overfitting in Machine Learning: A Comparative Analysis of Decision Trees and Random Forests.," *Intell. Autom. Soft Comput.*, vol. 39, no. 6, 2024.

[68] J. L. Speiser, M. E. Miller, J. Tooze, and E. Ip, "A comparison of random forest variable selection methods for classification prediction modeling," *Expert Syst. Appl.*, vol. 134, pp. 93–101, 2019.

[69] A. Razaque, M. Ben Haj Frej, M. Almi'ani, M. Alotaibi, and B. Alotaibi, "Improved support vector machine enabled radial basis function and linear variants for remote sensing image classification," *Sensors*, vol. 21, no. 13, p. 4431, 2021.

[70] D. Valero-Carreras, J. Alcaraz, and M. Landete, "Comparing two SVM models through different metrics based on the confusion matrix," *Comput. Oper. Res.*, vol. 152, p. 106131, 2023.

[71] R. K. Halder, M. N. Uddin, M. A. Uddin, S. Aryal, and A. Khraisat, "Enhancing K-nearest neighbor algorithm: a comprehensive review and performance analysis of modifications," *J. Big Data*, vol. 11, no. 1, p. 113, 2024.

[72] A. P. Salim, K. A. Laksitowening, and I. Asror, "Time series prediction on college graduation using kNN algorithm," in *2020 8th International Conference on Information and Communication Technology (ICoICT)*, IEEE, 2020, pp. 1–4.

[73] A. Shahraki, M. Abbasi, and Ø. Haugen, "Boosting algorithms for network intrusion detection: A comparative evaluation of Real AdaBoost, Gentle AdaBoost and Modest AdaBoost," *Eng. Appl. Artif. Intell.*, vol. 94, p. 103770, 2020.

[74] N. Cahyana, S. Khomsah, and A. Aribowo, "Improving Imbalanced Dataset Classification Using Oversampling and Gradient Boosting," in *2019 5th International Conference on Science in Information Technology (ICSITech)*, 2019, pp. 217–222.

[75] L. Pan, P. Zhang, C. Daengngam, S. Peng, and M. Chongcheawchamnan, "A review of artificial intelligence methods combined with Raman spectroscopy to identify the composition of substances," *J. Raman Spectrosc.*, vol. 53, no. 1, pp. 6–19, 2022.

[76] I. Riadi, R. Umar, and R. Anggara, "Comparative analysis of Naive Bayes and K-NN approaches to predict timely graduation using academic history," *Int. J. Comput. Digit. Syst.*, 2024, [Online].

[77] M. Maniruzzaman, M. A. M. Hasan, N. Asai, and J. Shin, "Optimal channels and features selection based ADHD detection from EEG signal using statistical and machine learning techniques," *IEEE Access*, vol. 11, pp. 33570–33583, 2023.

[78] A. Rahman *et al.*, "Multimodal EEG and keystroke dynamics based biometric system using machine learning algorithms," *IEEE Access*, vol. 9, pp. 94625–94643, 2021.

[79] R. Scheda and S. Diciotti, "Explanations of machine learning models in repeated nested cross-validation: an application in age prediction using brain complexity features," *Appl. Sci.*, vol. 12, no. 13, p. 6681, 2022.

[80] Y. Rimal, N. Sharma, and A. Alsadoon, "The accuracy of machine learning models relies on hyperparameter tuning: student result classification using random forest, randomized search, grid search, bayesian, genetic, and optuna algorithms," *Multimed. Tools Appl.*, vol. 83, no. 30, pp. 74349–74364, 2024.

[81] D. M. Alghazzawi, A. G. A. Alquraishee, S. K. Badri, and S. H. Hasan, "ERF-XGB: Ensemble random forest-based XG boost for accurate prediction and classification of e-commerce product review," *Sustainability*, vol. 15, no. 9, p. 7076, 2023.

[82] A. Biglari and W. Tang, "A review of embedded machine learning based on hardware, application, and sensing scheme," *Sensors*, vol. 23, no. 4, p. 2131, 2023.